J. Plasma Physics (2012), vol. 78, part 4, pp. 413–419. © Cambridge University Press 2012
doi:10.1017/S002237781200030X

Self-injected petawatt laser-driven plasma electron acceleration in 10^{17} cm^{-3} plasma

X. WANG, R. ZGADZAJ, S. A. YI, V. KHUDIK, W. HENDERSON, N. FAZEL, Y.-Y. CHANG, R. KORZEKWA, H.-E. TSAI, C.-H. PAI, Z. LI, E. GAUL, M. MARTINEZ, G. DYER, H. QUEVEDO, A. BERNSTEIN, M. DONOVAN, G. SHVETS, T. DITMIRE and M. C. DOWNER

Department of Physics, University of Texas at Austin, Austin, TX 78712, USA
(downer@physics.utexas.edu)

(Received 15 November 2011; revised 25 January 2012; accepted 26 January 2012; first published online 12 April 2012)

Abstract. We report production of a self-injected, collimated (8 mrad divergence), 600 pC bunch of electrons with energies up to 350 MeV from a petawatt laser-driven plasma accelerator in a plasma of electron density $n_e = 10^{17}$cm^{-3}, an order of magnitude lower than previous self-injected laser-plasma accelerators. The energy of the focused drive laser pulse (150 J, 150 fs) was distributed over several hot spots. Simulations show that these hot spots remained independent over a 5 cm interaction length, and produced weakly nonlinear plasma wakes without bubble formation capable of accelerating pre-heated (∼1 MeV) plasma electrons up to the observed energies. The required pre-heating is attributed tentatively to pre-pulse interactions with the plasma.

1. Introduction

Electric fields in laser-driven plasma accelerators (LPAs) reach ∼100 GV/m, three orders of magnitude larger than fields in conventional radio frequency (RF) linear accelerators, enabling extremely compact accelerator structures (Tajima and Dawson 1979). Recent LPA experiments have yielded quasi-monoenergetic, collimated, near-GeV electron beams with the help of self-guiding (Froula et al. 2009; Kneip et al. 2009) or preformed plasma channels (Leemans et al. 2006) to extend the acceleration length beyond the Rayleigh range of the focused drive laser pulse. In these experiments, ultra-intense (10^{19} Wcm^{-2}) laser pulses interacted with under-dense plasma of electron density $n_e \sim 10^{18}$–10^{19} cm^{-3} in the so-called blowout regime (Lu et al. 2006) to produce a highly nonlinear plasma wake, or bubble. Plasma electrons self-injected at the tail of the plasma bubble, and were then captured, focused and accelerated inside the bubble (Rosenzweig et al. 1991). For plasmas of density $n_e > 10^{18}$ cm^{-3}, the plasma period ω_p^{-1} is matched to sub-100 fs drive pulses, which require multi-TW, but sub-PW peak power to exceed the critical power $P_{\rm cr} = 17(n_{cr}/n_e)$ GW for relativistic self-focusing needed to self-guide (here $P_{\rm cr}$ is the critical density) and form bubbles. Moreover, surrounding plasma electrons readily self-inject into the accelerator structure at these densities (Froula et al. 2009; Kneip et al. 2009). On the other hand, output energy is limited to $\leqslant$1 GeV by the dephasing length $L_d = \gamma_\phi^2 \lambda_p$ (where $\lambda_p = 2\pi c/\omega_p$ is a plasma wavelength) over which injected electrons outrun the accelerating quadrant of plasma wakes propagating at phase velocity corresponding to Lorentz factor γ_ϕ^2, and by the drive pulse depletion length $L_{\rm dp} = (n_e/n_{\rm cr})c\tau_{\rm FWHM}$, where $\tau_{\rm FWHM}$ is the full-width at half-maximum of the initial drive pulse temporal profile.

A necessary condition for scaling LPAs to multi-GeV energies is to increase L_d and $L_{\rm dp}$ to longer (multi-cm) lengths. This in turn requires reducing plasma density well below $n_e \sim 10^{18}$ cm^{-3} (Lu et al. 2007). Such low densities, however, raise new challenges for LPA. For example, at $n_e = 10^{17}$ cm^{-3}, peak laser power $P \sim 1$ PW is now required to exceed $P_{\rm cr}$ and maintain self-guiding. Moreover, pulse duration $\tau_{\rm FWHM} \sim 150$ fs is needed to match ω_p^{-1}, as needed for efficient plasma wake generation. Pulse energy $E \sim 150$ J is therefore needed, necessitating in turn a significantly larger laser system than for previous experiments. Fortunately, such systems are now becoming available, and the Texas petawatt laser (Gaul et al. 2010) in particular meets the basic pulse requirements ($\tau_{\rm FWHM} \sim 150$ fs, $E \sim 150$ J) for LPA at $n_e = 10^{17}$ cm^{-3} almost perfectly. The increasing difficulty of electron self-injection at low plasma density then becomes the dominant technical problem for multi-GeV LPA. For previous experiments with sub-PW laser pulses, the threshold density for electron self-injection into LPAs is reported to be $n_e \sim 3 \times 10^{18}$ cm^{-3} (Froula et al. 2009). At lower density, fully blown out bubbles of larger radius R_b are required (Kostyukov et al. 2009; Lu et al. 2007). For experiments in which the focused e^{-2} laser spot size w_0 is matched to plasma density, $R_b \sim w_0 \sim 2k_p^{-1}\sqrt{a_0}$, where a_0 is the normalized vector potential, and $a_0 > 2$ is required in 3D to form a fully

https://doi.org/10.1017/S002237781200030X Published online by Cambridge University Press

blown out bubble. The twin requirements of larger w_0 and larger a_0 further amplify the need for PW drive laser pulses.

Two strategies for reducing the threshold density for efficient electron self-injection below the theoretical limits set by Froula et al. (2009) have recently been explored. In one of these, the fully ionized low-Z plasma assumed in Ref. Froula et al. (2009) is doped with a few percent of high-Z impurity gas (Pak et al. 2010; Pollock et al. 2011). Inner shell electrons of the dopant remain bound until the peak of the drive laser pulse, whereupon they are released into the plasma bubble, trapped and accelerated. Such ionization-induced injection has recently yielded electrons up to 1.5 GeV in plasma of density as low as 10^{18} cm^{-3} (Clayton et al. 2010). In the second approach (Kalmykov et al. 2009), an incident PW drive laser (~150 J, ~150 fs) is focused to a spot size that is NOT matched to the plasma density, causing it to over-self-focus and induce one or more periods of damped oscillation in R_b. Simulations show that this dynamics can self-inject electrons into bubbles formed in fully ionized low-Z plasma with density as low as $n_e \sim 2.5 \times 10^{17}$ cm^{-3}, resulting in quasi-monoenergetic acceleration up ~7 GeV over 10 cm (Kalmykov et al. 2010).

In this paper, we report the results of our initial LPA experiment with the Texas petawatt laser. Ultimately, these experiments are designed to explore the dynamically self-injected bubble regime of LPA treated in Kalmykov et al. (2010). Initial experiments, however, fell well short of this regime because the 150 J energy of the incident 150 fs, 1 μm pulses focused at f-number 40 was distributed over five to six hot spots within a total area of 200 μm × 300 μm, rather than concentrated in a single Gaussian spot of $w_0 < 100$ μm as anticipated in Kalmykov et al. (2010). In addition, temporal pre-pulses were present. Consequently, only mildly relativistic peak laser intensity ~10^{18} Wcm^{-2} was obtained, ruling out both bubble formation and self-guiding. Nevertheless, we observed the production of a self-injected ~600 pC bunch of electrons that were accelerated up to ~350 MeV as a result of the drive pulse interacting with a 5-cm-long pure He plasma of density $n_e = 10^{17}$ cm^{-3}. This is one order of magnitude lower than reported electron self-injection thresholds in previous experiments. The generated electron beam had continuous energy spectrum, and <8 mrad angular divergence. In view of the non-ideal pulse parameters described above, the injection and acceleration mechanisms appear to be quite different from those discussed in recent literature. Section 2 presents the experimental procedure and results. Section 3 presents simulations of the experiment using the particle-in-cell (PIC) code WAKE. The simulations show that the observed electron spectrum is consistent with acceleration of pre-heated plasma electrons by the mildly nonlinear plasma wake expected from the actual focused pulse. Possible pre-heating mechanisms are briefly discussed. The observation of efficient self-injection at such low plasma density is a promising first step towards achieving multi-GeV LPAs in tenuous plasma.

2. Experimental procedure and results

The Texas Petawatt Laser achieves an amplified pulse bandwidth of ~15 nm at centre wavelength 1057 nm by using a front-end optical parametric chirped pulse amplifier (OPCPA) followed by a mixture of phosphate and silicate Nd: glass final amplifiers. The results reported here were based on a run in which 20 full-system shots with energy 150 ± 13 J were delivered to the interaction region. The fully amplified pulses were focused through the 1-mm-diameter entrance aperture of He gas cell by an f/40 spherical mirror, resulting in a vacuum Rayleigh range $z_R \sim 2$ cm. Transverse spatial intensity profiles at the focus were acquired on every shot by imaging the focal plane profile of light leaked through a mirror in the main pulse delivery line after it was sent through an equivalent focus. Focused profiles of pulses used for the present results typically showed several hot spots, each containing 15% of the total pulse energy within e^{-2} width $w_0 \sim 80$ μm, as illustrated in Fig. 1(a). Temporal intensity profiles were also measured from leakage light on every shot with a single-shot autocorrelator. Figure 1(b) shows an autocorrelation trace corresponding to FWHM ~150 fs for the same pulse that yielded the spatial profile in Fig. 1(a). Based on the combined measurements, the maximum focused intensity in each hot spot in Fig. 1(a) was ~1.2×10^{18} Wcm^{-2} ($a_0 \sim 1$). The FWHM of pulses in this run varied from ~130 fs to over 500 fs. Electrons were observed only for pulses with FWHM < 180 fs that was approximately resonant with ω_p^{-1}. In future runs, an adaptive optic system will be used to improve the focal spot quality and the consistency of delivered pulse duration.

Figure 2 illustrates the schematic experimental set-up. The PW laser pulse enters a 5 cm long gas cell with its waist at the entrance aperture, and exits the cell through a 2-mm-diameter aperture after interacting with the gas. The transmitted pulse is deflected to a beam dump by a 0.8 mm thick, 8 cm × 70 cm aluminium foil stretched over a metal frame that is located 1.5 m downstream from the gas cell exit aperture and tilted with its surface normal at 83° to the laser pulse propagation direction. No ablation of this film was observed for full-system PW shots. The film transmits >500 MeV electrons with negligible energy loss.

Pure He gas flowed into the cell within ~5 ms via an intermediate ballast chamber, then leaked out through the entrance and exit apertures over ~50 ms. Peak density was controlled by adjusting the opening time of a solenoid valve in the gas fill line and the backing pressure. Gas pressure in the interaction chamber was monitored with 0.1 ms time resolution by an ultrafast miniature pressure sensor (Entran Part No. EPE-T21-0.13B-/M/Z2/V05/L02F; pressure range 0-100 Torr

https://doi.org/10.1017/S002237781200030X Published online by Cambridge University Press

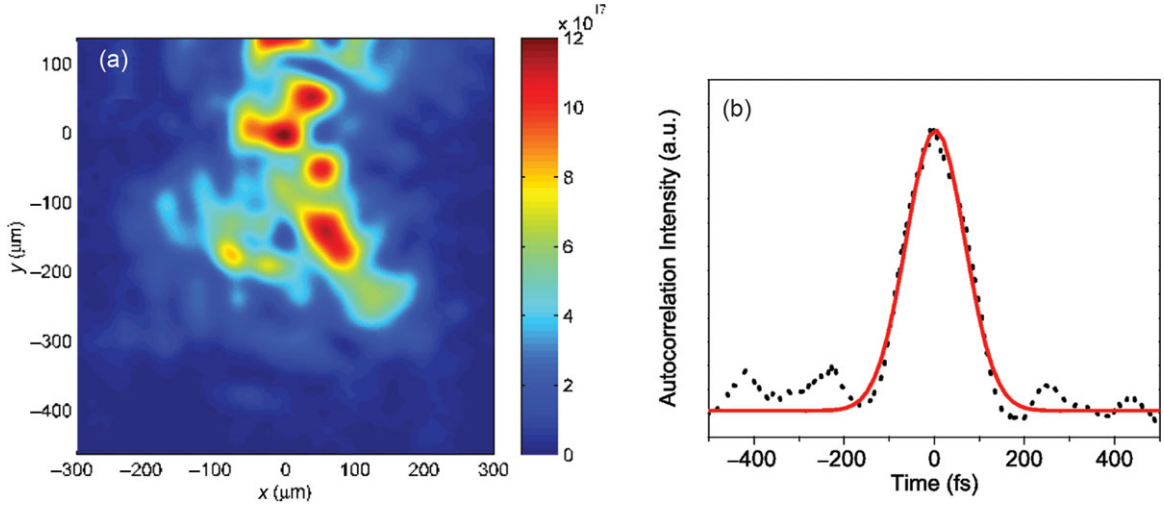


Figure 1. PW laser beam quality and pulse duration. (a) Focused intensity profile in $I(\mathrm{Wcm}^{-2})$, (b) single-shot autocorrelation trace.

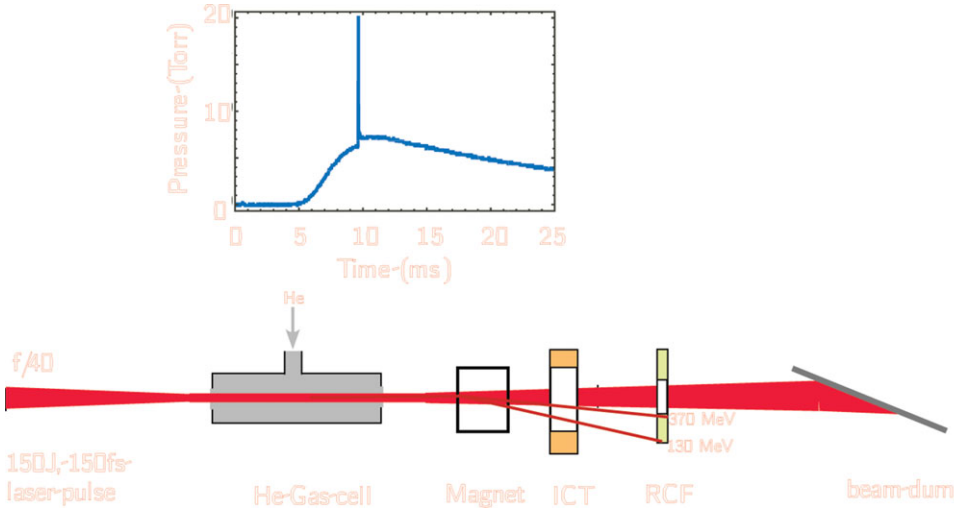


Figure 2. Schematic of Texas petawatt laser wakefield acceleration experiments. ICT detects electrons with energy over 65 MeV and RCF detects electron energy ranging from 130 to 350 MeV. The inset shows a typical pressure vs. time curve.

and frequency = 80 kHz) that was pre-calibrated for measurements in the pressure range corresponding to plasma densities $1–5 \times 10^{17}$ cm^{-3} of doubly ionized He. The inset of Fig. 2 shows a typical pressure vs. time curve. These curves provided the basis for timing arrival of the PW pulse to coincide with a pre-set gas density.

A 1.1 Tesla, 5×5 cm dipole magnet located 18 cm downstream from the gas cell deflected the generated electrons beams. An integrating current transformer (ICT) immediately after the magnet recorded the total charge of the accelerated electrons. Electrons with energies ranging from 130 to 350 MeV were recorded on a sheet of Gafchromic EBT2 radiochromic film (RCF) in the shape of an annulus located 40 cm from the gas cell exit, with the central hole cut to allow passage of the transmitted drive pulse. The RCF was covered with aluminium foil on both sides to shield it from scattered PW laser light. Additional detectors (not shown) were set up downstream from the aluminium deflector to record electrons with energy > 500 MeV that passed through the central hole in the RCF and the deflector foil. However, no electrons were observed in this range in the present run.

Figure 3 shows an RCF recording of the electron energy spectrum generated by the PW laser shot profiled in Fig. 1 as a result of interacting with plasma of density $n_e = 1 \times 10^{17}$ cm^{-3}. The electron energy varies continuously from 130 ± 20 to 350 ± 50 MeV, with more electrons at lower energy than higher energy. The upper end of the spectrum was limited by the size of the laser transmission hole in the RCF, so it is possible that some electrons with energies up to 500 MeV were also generated. The vertical spread of electron positions on the RCF recording corresponds to an angular divergence of ± 4 mrad. The RCF signal was read with a commercial scanner, whose sensitivity was calibrated prior to scanning. The response of the RCF itself is well documented by the manufacturer and

https://doi.org/10.1017/S002237781200030X Published online by Cambridge University Press

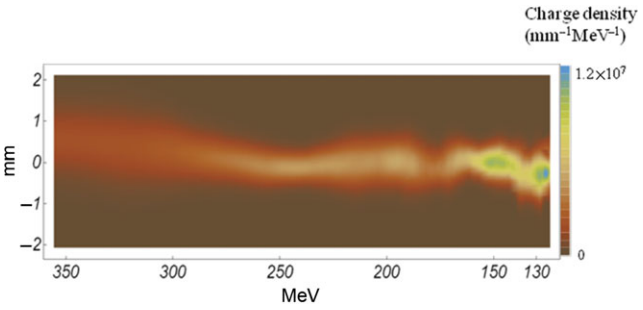


Figure 3. Energy spectrum of electron beam generated by LPA with a PW laser shot at $n_e = 10^{17}\text{cm}^{-3}$, recorded with RCF 40 cm away from gas cell exit.

in literature. The small signal and the graininess of the film resulted in a noisy signal which was smoothed by performing Gaussian fits to the transverse cross section of the dispersed electron beam image and by locally averaging several pixels in the longitudinal direction. The total electron charge obtained from integrating the calibrated RCF signal is ~40 pC, whereas the ICT measured 600 pC for this shot. The discrepancy arises because RCF does not record electrons with energies <130 MeV or >350 MeV. Evidently, the lower energy electrons dominate the ICT signal.

3. Simulations

Due to the presence of multiple hot spots in the focused laser pulse, it is important to understand whether these spots each interact with the plasma separately, or merge due to self-focusing. If the hot spots do not merge, then it is sufficient to simulate the interaction between a single hot spot and the plasma. To determine whether the spots collapse into each other, we start with the wave equation that describes the laser propagation (Antonsen and Mora 1993)

$$\left(\nabla^2 - \frac{1}{c^2}\frac{\partial^2}{\partial t^2}\right)\mathbf{a} = k_p^2\left(1 + \frac{\delta n}{n_0} - \frac{1}{2}\left\langle|\mathbf{a}|^2\right\rangle\right)\mathbf{a}, \qquad (3.1)$$

where $\mathbf{a} = e\mathbf{A}(\mathbf{x},t)/(mc^2)$ is the normalized vector potential. The term $\delta n/n_0$ represents the plasma density perturbation, and $\langle|\mathbf{a}|^2\rangle$ represents the relativistic correction to the electron motion, valid in the mildly relativistic limit. Ignoring the contribution from the plasma density perturbation and taking the paraxial approximation leads to the well-known nonlinear Schrodinger equation, which has the conserved quantity (Vlasov et al. 1971)

$$I \equiv \int\left(|\nabla_\perp a|^2 - \frac{k_p^2}{8}|a|^4\right)d\mathbf{x}_\perp. \qquad (3.2)$$

From Vlasov et al. (1971), if $I < 0$ the laser has enough power for a relativistic "collapse", and the hot spots will all merge into one. We have confirmed the validity of this condition using PIC simulations: a distribution with $I < 0$ leads to self-focusing in the corresponding simulation, whereas $I > 0$ leads to diffraction.

The laser intensity distribution at focal plane (as shown in Fig. 1) has been smoothed using a fast Fourier transform (FFT) low-pass filter to facilitate the numerical transverse derivative in (1). Evaluating the integral in (3.2) for this distribution and the plasma density $n_0 = 10^{17}$ cm^{-3} gives $I > 0$, so that the hot spots do not collapse into each other. Thus, in the following simulations, we model the interaction of one of the laser hot spots with the plasma.

We performed simulations of the laser wakefield structure and evolution using the PIC code WAKE (Mora and Antonsen 1997). WAKE simulates the laser–plasma interaction in a cylindrically symmetric geometry using two different types of particles. Macroparticles are self-consistently treated using the quasi-static approximation, which prevents them from becoming self-injected. To test for injection, test particles that are unrestricted by the quasi-static approximation are used. The laser pulse acts on both types of particles through the time-averaged ponderomotive force, and propagates through an extended paraxial wave equation (with group velocity dispersion taken into account).

The laser pulse in our WAKE simulation was Gaussian in both longitudinal and transverse directions, with $I = 1.65 \times 10^{18}$ W/cm^2, $w_0 = 85\,\mu$m spot size and 130 fs FWHM pulse length. A 5 cm long pre-ionized plasma of density $n_0 = 10^{17}$ cm^{-3} was assumed, with 0.5 cm linear density ramps at entrance and exit. Given these conditions, $a_0 \approx 1.15$ and $P/P_{\text{cr}} \approx 1.2$. Our simulations indicate that for such a tenuous plasma, self-focusing is insignificant and the laser pulse gradually diffracts over the length of the plasma. A mildly nonlinear plasma wake is formed, with no indication of bubble formation.

Simulations of electron self-injection were performed using WAKE test particles. We found that initially quiescent electrons, i.e. test particles seeded at rest in the lab frame, were not injected into the wake. However, when electrons were pre-heated to 1 MeV, some of them were self-injected and accelerated over the 5 cm plasma length. Figure 4 illustrates this injection mechanism. Figure 4(a) snapshot near the beginning of the laser–plasma interaction shows plasma electron density in the top half, and pre-heated test electrons moving left (in the direction of laser propagation) in red in the bottom half. As the pre-heated electrons begin to interact with the pump pulse and wake, some of them are self-injected into the first accelerating bucket. These injected electrons obtain energies of up to 370 MeV at the plasma exit, as shown in red in Fig. 4(b).

The most likely mechanism for pre-acceleration at this low-density is one colliding pulse interaction involving pre- or post-pulses. Weak ($a_0 \leqslant 0.1$) pulses that counter-propagate with the main pulse can be generated by accidental reflection from debris within the cell or from the cell apertures, or for pre-pulses of length $ct_p > \lambda_p$, by Raman backscatter (RBS). Pre- and post-pulses were known to be present — indeed some are evident in the autocorrelation trace in Fig. 1(b) — but were

https://doi.org/10.1017/S002237781200030X Published online by Cambridge University Press

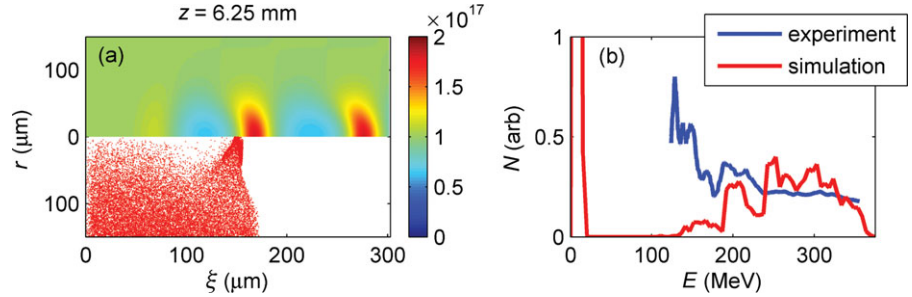


Figure 4. Injection of pre-heated 1 MeV electrons into an evolving weakly-nonlinear wake (no bubble). (a) Plasma electron density (top half) and pre-heated electrons (bottom half). Laser propagation is to the left. (b) Electron energy spectrum at plasma exit ($z = 5\,\mathrm{cm}$).

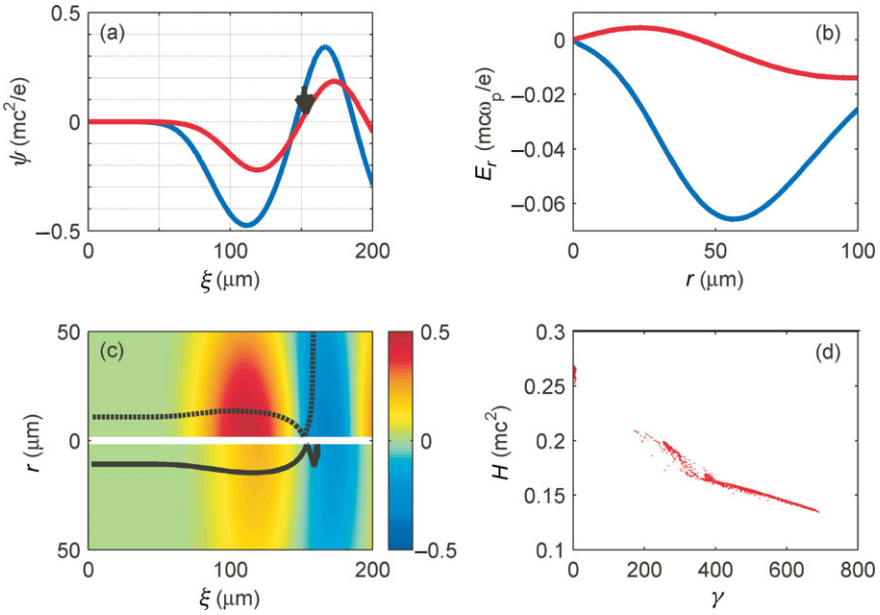


Figure 5. (Colour online) Injection of pre-heated electrons due to evolution of the weakly-nonlinear wake. (a) On-axis wake potential $\psi \equiv A_z - \phi$ at the beginning (blue line) and at the end (red line) of the plasma. The wake's amplitude/phase changes due to the diffraction/slippage of the laser pulse. Accelerated electrons are injected at position ξ_{inj}, where ψ is reduced to $\psi(\xi_{\mathrm{inj}}) = 0.22\,mc^2/e$. (b) Radial line-outs of the focusing field $E_r = \partial\psi/\partial r$ (normalized to $mc\omega_p/-e$) at ξ_{inj} at the beginning of the plasma (blue) and the end of the plasma (red). (c) Wake potential ψ for frozen (upper half) and evolving (lower half) laser pulses, with the corresponding typical trajectories of scattered (dashed black) and injected (solid black) pre-heated electrons with the same initial energy $\gamma_0 mc^2 = 1\,\mathrm{MeV}$ and impact parameter $r_0 = 9\,\mu\mathrm{m}$. (d) Moving-frame Hamiltonian H of the pre-heated electrons versus γ at the end of the plasma. High-energy injected electrons have experienced a reduction in H due to wake evolution.

not characterized in detail. Thus, the precise colliding pulse responsible for pre-heating cannot be identified with certainty. Nevertheless, there are several plausible scenarios. For example, RBS of a long pre-pulse results in beating between the RBS light and the forward-propagating pre-pulse, creating a slow forward-moving beatwave that can pre-accelerate electrons (Esarey and Sprangle 1992; Moore et al. 1997). The growth rate $\Gamma/\omega_0 \sim (\omega_p/\omega_0)^{2/3}$ (Esarey and Sprangle 1992) for RBS scales weakly with plasma density, making this a plausible mechanism at our low densities. RBS, or accidental back-reflection, of the pre-pulse, or back-reflection of one of the neighbouring hot spots of the main pulse (see Fig. 1(a)), can also beat with the main pulse, resulting in stochastic heating of plasma electrons (Sheng et al. 2002). With a main pulse of $a_0 \sim 1.2$, a back-reflected pulse of $a_1 \sim 0.1$ would be adequate to pre-heat electrons to $\sim$1 MeV (Sheng et al. 2002). Yet another scenario is that an accidental back-reflection of the main pulse collides with a short post-pulse within the wake created by the main pulse. The colliding-pulse interaction creates a slow ponderomotive beatwave that can inject electrons into the wake (Esarey et al. 1997). This mechanism is also compatible with our low densities.

Numerical simulations indicate that evolution of the laser pulse and the wakefield is crucial to the self-injection (Kalmykov et al. 2009; Yi et al. 2011) observed above. Repeating the above simulation, but with the laser pulse artificially "frozen" (i.e. propagating with constant group velocity v_g and amplitude a_0)), we did not observe any significant acceleration of 1 MeV pre-heated electrons. Figure 5 illustrates the role of the dynamic wake in the injection process. Specifically, the axial

https://doi.org/10.1017/S002237781200030X Published online by Cambridge University Press

line-out of wake's pseudo-potential $\psi \equiv A_z - \phi$ which governs the acceleration and transverse focusing/defocusing of a relativistic electron bunch (Yi et al. 2011) is shown in Fig. 5(a) at the beginning (blue line) and at the end (red line) of the plasma. The slow diffraction of the laser pulse has two effects: reduction of the wake density perturbation, and modification of the laser group velocity characterized by $\gamma_g = 1/\sqrt{1 - v_g^2/c^2}$ and given by (Esarey and Leemans 1999)

$$\gamma_g \approx \left(\omega_p^2/\omega_0^2 + 2c^2/\omega_0^2 w_0^2\right)^{-1/2}. \quad (3.3)$$

Note that for tightly focused laser pulses, the second term in (3.3) can be comparable with the first one, thereby further depressing the group velocity of the laser pulse. and the phase velocity of the wake. Since the phase velocity of the wake is $v_0 \approx v_g$ (Esarey et al. 2009), the wake potential slips backward with respect to the speed-of-light coordinate $\xi = ct - z$, while also decreasing in amplitude. The reduction of the wake's amplitude $|\psi|$ and phase manifest in the change of the moving-frame Hamiltonian (Mora and Antonsen 1997) given by

$$H = mc^2\sqrt{1 + (\mathbf{P}/mc + |e|\mathbf{A}/mc^2)^2} - v_0 P_z - |e|\phi \quad (3.4)$$

$$\approx mc^2\gamma - v_0 p_z + |e|\psi \quad (3.5)$$

as shown in Fig. 5(d). It has been shown (Kalmykov et al. 2009; Yi et al. 2011) that such reduction is crucial for self-injection of initially quiescent plasma electrons into highly nonlinear plasma bubbles. However, the effect of the evolution of a weakly-nonlinear plasma wake on the injection of pre-heated electrons has not been examined. Based on numerical simulation and theoretical arguments presented below, we believe that this effect was indeed observed in the Texas petawatt experiment.

Even without evolution of the wake, injection of pre-heated electrons is, in principle, possible because the initial moving-frame Hamiltonian $H_0 \approx 0.265mc^2$ and the peak of the plasma wake's potential $\psi_{\max} \approx 0.34mc^2/e$ satisfy the $H_0 < \psi_{\max}$ condition that corresponds to one-dimensional bouncing of an electron off the wake. In practice, the radial component of the wakefield at the injection phase $\xi_{\rm inj}$ (approximately defined by $\psi(\xi_{\rm inj}) = H_0$) is defocusing as illustrated by the blue line in Fig. 5(b). Therefore, in a non-evolving wake, the potentially self-injected electrons are transversely scattered by the wake as illustrated in the top panel of Fig. 5(c).

If, on the other hand, the electrons are pre-accelerated to 2.6 MeV, corresponding to an initial moving-frame Hamiltonian $H_0^* = 0.1mc^2$, the transverse fields are focusing at the position ξ^*, where $\psi(\xi^*) = H_0^*$. In this case, continuous injection occurs for a frozen wake, leading to a flat electron energy spectrum at the end of the plasma. Since such an energy spectrum is inconsistent with the experimental data in Fig. 4(b), we conclude that this type of injection was not the one observed in experiment. We note that this type of injection is only possible in the case of a nonlinear wake, because for a linear wake, there are no regions where both $\psi > 0$ and the transverse fields are focusing.

The situation changes dramatically for an evolving wake, where the moving-frame Hamiltonian is reduced from its initial value of H_0 as shown in Fig. 5(d). In this evolving case, the transverse force becomes focusing at $\xi_{\rm inj}$, as illustrated by the red line in Fig. 5(b). The trajectory of a typical self-injected pre-heated electron (solid black line) is shown in Fig. 5(c), superimposed on a colour plot of the wake potential ψ. Therefore, the reduction of the moving-frame Hamiltonian is responsible for the electron injection, where there would otherwise be transverse deflection. We conclude that the evolution of the wake plays a critical role in facilitating the self-injection, into a realistic weakly-nonlinear 3-D wake, consistent with previous findings (Kalmykov et al. 2009; Yi et al. 2011).

4. Conclusion

We demonstrate self-injected laser–plasma acceleration of electrons up to 350 MeV in plasma of density $n_e = 10^{17}\,{\rm cm}^{-3}$, 10 times lower than previous self-injected LPA experiments. The 150 J energy of the 150 fs drive laser pulse from the Texas PW laser was distributed over several hot spots, each of which reached only weakly relativistic intensity ($a_0 \sim 1.2$). Simulations show that, as a result, plasma bubbles did not form, individual sub-pulses did not self-guide, and injection could occur only if background plasma electrons were pre-heated to $\sim$1 MeV — e.g. by a colliding pulse interaction involving backscattered or reflected pre- or post-pulses — and if the weakly nonlinear wake evolved in shape while interacting with the pre-heated electrons. Under these conditions, the simulations reproduce the observed electron energy spectrum reasonably well. Demonstration of self-injected LPA at such low density is a stepping-stone toward production of multi-GeV electrons. In future, LPA experiments with the Texas petawatt Laser, the focal spot quality will be improved with adaptive optics. It should then become possible to realize self-guided, self-injected LPA up to several GeV in low-density plasma, as predicted by earlier simulations (Kalmykov et al. 2010).

Acknowledgements

This work was supported by DoE grants DE-FG03-96ER40954, DE-FG02-07ER54945 and DE-FG02-04ER41321, NSF grant PHY-0936283 and DoE NNSA under Cooperative agreement DE-FC52-03NA00156.

References

Antonsen, T. M., Jr. and Mora, P. 1993 Self-focusing and Raman scattering of laser pulses in tenuous plasmas. *Phys. Fluids* B **5**, 1440–1452.

https://doi.org/10.1017/S002237781200030X Published online by Cambridge University Press

Clayton, C. E., Ralph, J. E., Albert, F., Fonseca, R. A., Glenzer, S. H., Joshi, C., Lu, W., Marsh, K. A., Martins, S. F., et al. 2010 Self-guided laser wakefield acceleration beyond 1 Gev using ionization-induced injection. *Phys. Rev. Lett.* **105**, 105003.

Esarey, E., Hubbard, R. F., Leemans, W. P., Ting, A. and Sprangle, P. 1997 Electron injection into plasma wakefields by colliding laser pulses. *Phys. Rev. Lett.* **79**, 2682–2685.

Esarey, E. and Leemans, W. P. 1999 Nonparaxial propagation of ultrashort laser pulses in plasma channels. *Phys. Rev.* E **59**, 1082–1095.

Esarey, E., Schroeder, C. B. and Leemans, W. P. 2009 Physics of laser-driven plasma-based electron accelerators. *Rev. Mod. Phys.* **81**, 1229–1285.

Esarey, E. and Sprangle, P. 1992 Generation of stimulated backscattered harmonic radiation from intense-laser interactions with beams and plasmas. *Phys. Rev.* A **45**, 5872–5882.

Froula, D. H., Clayton, C. E., Doppner, T., Marsh, K. A., Barty, C. P. J., Divol, L., Fonseca, R. A., Glenzer, S. H., Joshi, C., Lu, et al. 2009 Measurements of the critical power for self-injection of electrons in a laser wakefield accelerator. *Phys. Rev. Lett.* **103**, 215006.

Gaul, E. W., Martinez, M., Blakeney, J., Jochmann, A., Ringuette, M., Hammond, D., Borger, T., Escamilla, R., Douglas, S., et al. 2010 Demonstration of a 1.1 petawatt laser based on a hybrid optical parametric chirped pulse amplification/mixed Nd:glass amplifier. *Appl. Opt.* **49**(9), 1676–1681.

Kalmykov, S. Y., Yi, S. A., Beck, A., Lifschitz, A. F., Davoine, X., Lefebvre, E., Pukhov, A., Khudik, V., Shvets, G., et al. 2010 Numerical modelling of a 10-cm-long multi-gev laser wakefield accelerator driven by a self-guided petawatt pulse. *New J. Phys.* **12**(4), 045019.

Kalmykov, S., Yi, S. A., Khudik, V. and Shvets, G. 2009 Electron self–injection and trapping into an evolving plasma bubble. *Phys. Rev. Lett.* **103**, 135004.

Kneip, S., Nagel, S. R., Martins, S. F., Mangles, S. P. D., Bellei, C., Chekhlov, O., Clarke, R. J., Delerue, N., Divall, E. J., et al. 2009 Near-Gev acceleration of electrons by a nonlinear plasma wave driven by a self-guided laser pulse. *Phys. Rev. Lett.* **103**, 035002.

Kostyukov, I., Nerush, E., Pukhov, A. and Seredov, V. 2009 Electron self-injection in multidimensional relativistic-plasma wake fields. *Phys. Rev. Lett.* **103**, 175003.

Leemans, W. P., Nagler, B., Gonsalves, A. J., Tóth, C., Nakamura, K., Geddes, C. G. R., Esarey, E., Schroeder, C. B. and Hooker, S. M. 2006 Gev electron beams from a centimetre-scale accelerator. *Nature Phys.* 696–699.

Lu, W., Huang, C., Zhou, M., Mori, W. B. and Katsouleas, T. 2006 Nonlinear theory for relativistic plasma wakefields in the blowout regime. *Phys. Rev. Lett.* **96**, 165002.

Lu, W., Tzoufras, M., Joshi, C., Tsung, F. S., Mori, W. B., Vieira, J., Fonseca, R. A. and Silva, L. O. 2007 Generating multi-Gev electron bunches using single stage laser wakefield acceleration in a 3d nonlinear regime. *Phys. Rev. ST Accel. Beams* **10**, 061301.

Moore, C. I., Ting, A., Krushelnick, K., Esarey, E., Hubbard, R. F., Hafizi, B., Burris, H. R., Manka, C. and Sprangle, P. 1997 Electron trapping in self–modulated laser wakefields by Raman backscatter. *Phys. Rev. Lett.* **79**, 3909–3912.

Mora, P. and Antonsen, T. M., Jr. 1997 Kinetic modeling of intense, short laser pulses propagating in tenuous plasmas. *Phys. Plasmas* **4**, 217–229.

Pak, A., Marsh, K. A., Martins, S. F., Lu, W., Mori, W. B. and Joshi, C. 2010 Injection and trapping of tunnel-ionized electrons into laser-produced wakes. *Phys. Rev. Lett.* **104**, 025003.

Pollock, B. B., Clayton, C. E., Ralph, J. E., Albert, F., Davidson, A., Divol, L., Filip, C., Glenzer, S. H., Herpoldt, K., et al. 2011 Demonstration of a narrow energy spread, ∼0.5 GeV electron beam from a two-stage laser wakefield accelerator. *Phys. Rev. Lett.* **107**, 045001.

Rosenzweig, J. B., Breizman, B., Katsouleas, T. and Su, J. J. 1991 Acceleration and focusing of electrons in two-dimensional nonlinear plasma wake fields. *Phys. Rev.* A **44**, R6189–R6192.

Sheng, Z.-M., Mima, K., Sentoku, Y., Jovanović, M. S., Taguchi, T., Zhang, J. and Meyer-ter Vehn, J. 2002 Stochastic heating and acceleration of electrons in colliding laser fields in plasma. *Phys. Rev. Lett.* **88**, 055004.

Tajima, K. and Dawson, J. 1979 Laser electron accelerator. *Phys. Rev. Lett.* **43**, 267–270.

Vlasov, S. N., Petrishchev, V. A. and Talanov, V. I. 1971 Averaged description of wave beams in linear and nonlinear media (the method of moments). *Radiophys. Quantum Electron.* **14**, 1062–1070.

Yi, S. A., Khudik, V., Kalmykov, S. Y. and Shvets, G. 2011 Hamiltonian analysis of electron self–injection and acceleration into an evolving plasma bubble. *Plasma Phys. Controlled Fusion* **53**, 014012.

https://doi.org/10.1017/S002237781200030X Published online by Cambridge University Press